Electrochimica Acta 115 (2014) 370–377

Contents lists available at ScienceDirect

Electrochimica Acta

journal homepage: www.elsevier.com/locate/electacta

Adsorption–desorption mechanism of a cationic polyelectrolyte based on dimethylaminoethyl polymethacrylates at the water/1,2-dichloroethane interface

Julieta S. Riva[a], Dante M. Beltramo[b], Lidia M. Yudi[a,*]

[a] Instituto de Investigaciones en Fisicoquímica de Córdoba, (INFIQC) CONICET and Departamento de Fisicoquímica, Facultad de Ciencias Químicas, Universidad Nacional de Córdoba, Ala 1, Pabellón Argentina, Ciudad Universitaria, 5000 Córdoba, Argentina
[b] Centro de Excelencia en Productos y Procesos de Córdoba (CEPROCOR), Ministerio de Ciencia y Tecnología de Córdoba, Pabellón CEPROCOR, Santa María de Punilla, Argentina and Consejo Nacional de Investigaciones Científicas y Técnicas, CONICET, Córdoba 5164, Argentina

ARTICLE INFO

Article history:
Received 24 July 2013
Received in revised form 19 October 2013
Accepted 21 October 2013
Available online 2 November 2013

Keywords:
Eudragit® E100
Polyelectrolytes
Liquid/liquid interfaces
Electrochemistry

ABSTRACT

The electrochemical behaviour of the cationic polymer Eudragit® E100 at the polarized water/1,2-dichloroethane interface was studied. The voltammetric response was found to be dependent on the pH of the aqueous phase solution, on the nature of the organic electrolyte, and it was also time dependent during multi-cyclic voltammetry experiments. The results suggest that a diffusion process coupled to an adsorption or re-arrangement of E100 molecules at the interface is taking place. From the analysis of the desorption process, it was determined the presence of a strong attractive interaction between the adsorbed species at the interface and the lateral interaction parameter was calculated.

1. Introduction

Polymethacrylates are polymers widely used for pharmaceutical applications, and are worldwide known in the industry under the trade name Eudragit®. They are copolymers derived from acrylic esters and methacrylic acid, whose physicochemical properties are determined by their functional groups.

The use of different types of Eudragit for controlled release of drugs has been known for several years. Some of them are polycations (Eudragit types E, RL, RS, NE) and other are polyanions (Eudragit L, S). The formers have positively charged groups such as: dimethylamino groups in Eudragit® type E, or quaternary amino groups in Eudragit® type RL, RS, and NE. The polyanions have carboxyl groups negatively charged for both Eudragit types, L and S [1,2].

Eudragit E100 polymer is a cationic copolymer based on 2-dimethylaminoethyl methacrylate, methylmethacrylate and *n*-butylmethacrylate. Its chemical structure is shown in Scheme 1. This polymer is soluble in weakly acidic buffers (to about pH 5.00), while its deprotonated form is soluble in organic solvents like isopropanol, acetone, methylene chloride, ethanol, methanol, it has low viscosity and good adhesion [3] and does not require addition of plasticizers, due to its high elasticity.

E100 is widely used in oral and topical formulations and is considered non-toxic, non-irritating, and essentially safe in humans [4,5]. It has been evaluated the performance of solid dispersions containing Eudragit and different drugs such as divalproex sodium [6], albendazole [7], piroxicam [8], lidocaine [9]. This polyelectrolyte has also been used for drug delivery systems in various transdermal systems [10].

It has also been shown that E100 interacts with negatively charged proteins, membranes and viral DNA, causing lysis of membranes and thus exerting antiviral and antifungal action [11,12]. For these reasons, the study of surface properties of these substances on diverse interfaces, employed for modeling biological membranes, has been a topic of growing interest. Among them we can mention the solid/liquid, the air/water and the liquid/liquid interfaces.

Recently, the interfacial behavior of several polyelectrolytes at liquid/liquid interfaces has been studied by different authors [13–20] and much attention has been paid to the investigation of biopolymers adsorption including a polysaccharide heparin [21–25], the proteins protamine [26–29], insulin [30], hemoglobin [31,32], myoglobin [33], mellitin [34], cytochrome c and ribonuclease A [29,35].

In order to contribute to the understanding of E100 surface activity, in the present paper we present the electrochemical

* Corresponding author. Tel.: +54 351 4334169 80, fax: +54 351 4334188.
E-mail addresses: mjudi@fcq.unc.edu.ar, mabelyudi@gmail.com (L.M. Yudi).

0013-4686/$ – see front matter © 2013 Elsevier Ltd. All rights reserved.
http://dx.doi.org/10.1016/j.electacta.2013.10.156

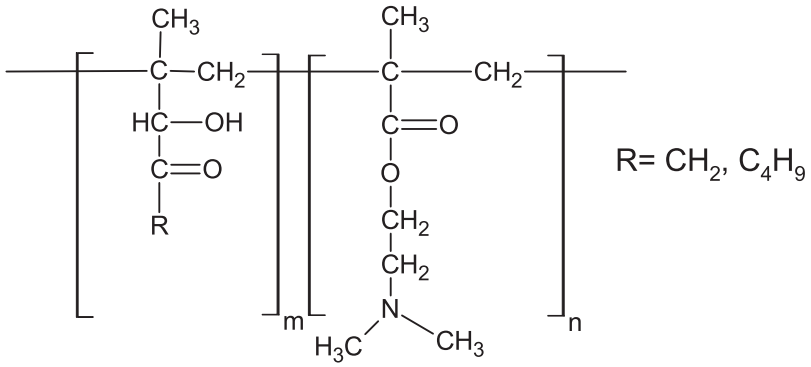

Scheme 1. Chemical structure of E100.

behavior of E100 at the polarized aqueous/organic interface. The study has been carried out employing cyclic voltammetry and electrochemical impedance spectroscopy and the mechanism proposed for the polymer transfer includes interfacial adsorption and diffusion processes. It is also shown that the adsorbed species exerts a strong attractive interaction between them.

2. Experimental

2.1. Materials and electrochemical cells

Eudragit® E100, aminoacrylmethacrylate copolymer, with an average molecular weight (MW) of 150 kDa, was a gift from Etilfarma S.A. (Buenos Aires, Argentina) and was used without further purification.

The base electrolyte solutions were 1.0×10^{-2} M LiCl (Merck p.a.) in ultrapure water (Milli-Q RiOs 16, Millipore) and 1.0×10^{-2} M tetraphenylarsonium dicarbollylcobaltate (TPhAsDCC) or 1.0×10^{-2} M tetrapentylammonium tetrakis (4-chlorophenyl) borate (TPnATClPhB) in 1,2-dichloroethane (DCE, Dorwil p.a.). TPhAsDCC and TPnATClPhB were prepared by metathesis of tetraphenylarsonium chloride (TPhAsCl, Sigma) and sodium dicarbollylcobaltate (NaDCC, Strem Chemicals) or tetrapentylammonium bromide (TPnABr, Fluka) and potassium tetrakis (4-chlorophenyl) borate (KTClPhB, Sigma-Aldrich), respectively. The precipitates were recrystallized from water: acetone mixtures and then dried in an oven at 30 °C for two days.

All experiments were performed in a four-electrode system using a conventional glass cell of 0.18 or 0.83 cm^2 interfacial area for voltammetric or electrochemical impedance spectroscopy experiments, respectively. In both cases, two platinum wires were used as counter-electrodes and the reference electrodes were Ag/AgCl, which were located in opposing phases, and controlled the applied potential across the liquid–liquid interface. The reference electrode in contact with the organic solution was immersed in an aqueous solution of 1.0×10^{-2} M TPhAsCl or 1.0×10^{-2} M TPnABr $+1.0 \times 10^{-2}$ M LiCl.

2.2. Methods

2.2.1. Cyclic voltammetry

Cyclic voltammetry and potential pulse experiments were carried out using a four-electrode potentiostat, which automatically eliminates the IR drop by means of a periodic current-interruption technique [36]. A wave potential generator (PPR1 Hi-Teck Instruments, UK) and a 10 bit Computer Boards acquisition card connected to a personal computer were also employed.

The potential values E reported in the voltammograms are the applied potentials between the two Ag | AgCl reference electrodes which are related to the Galvani potential difference ($\Delta_o^w\varphi$) across the interface by: $E = (\Delta_o^w\varphi) + \Delta E_{ref}$, where ΔE_{ref} depends on the reference electrodes and the reference solutions employed.

For cyclic voltammetry experiments, the polymer was added to the aqueous phase to final concentrations within the range between 0.020% and 0.100% w/v (equivalent to 1.33×10^{-6} and 6.67×10^{-6} M, respectively). Due to the presence of tertiary amines in these polymers, pH value determines the amount of protonated groups, so that, the pH of the aqueous phase was varied between 1.92 and 8.15 by addition of HCl (Merck p.a.) or LiOH (Merck pa), with the aim of analyzing the effect of the charge in the interfacial behavior of this polymer.

2.2.2. Electrochemical impedance spectroscopy

Electrochemical impedance spectroscopy experiments were carried out employing an Autolab potentiostat connected to a personal computer. An ac perturbation of amplitude 0.010 V and frequency scanned between 0.03 Hz to 3 kHz was applied to the interface at two different dc potential values, $E_{dc} = 0.450$ and 0.550 V. The collected data were fitted with several equivalent circuits, with the help of ZPLOT/ZVIEW software (Scribner Associates Inc.).

When performing Electrochemical Impedance Spectroscopy experiments, the polymer was added to the aqueous phase at concentration 0.020% w/v and pH = 3.00. The impedance spectra were recorded in the absence and presence of E100 in aqueous phase, before and after applying successive potential sweeps to the interface.

3. Results and discussion

3.1. Cyclic voltammetry

Fig. 1a and b shows the voltammetric profiles obtained when E100 was added to the aqueous phase at a concentration value equal to 0.100% w/v at pH = 3.00 and 5.00, respectively. It is worthwhile to remark the asymmetry in the general shape of the voltammetric profiles, with a broad forward peak and a comparatively much narrower reverse peak. Taking into account that these processes are not observed in the absence of E100, they can be attributed to the transfer of the cationic polyelectrolyte from the aqueous to the organic phase and the return of the polycation to the aqueous phase, respectively

Concerning to the positive peak, a linear behavior of peak current, $Ip(+)$, with the square root of sweep rate, $v^{1/2}$, was obtained at low pH values (shown in the inset graph in Fig. 1a), while a linear dependence of $Ip(+)$ with sweep rate, v, was observed at pH 5.00, (inset in Fig. 1b). These results are indicating the presence of a diffusion process at low pH values and an activation-controlled interfacial adsorption mechanism at higher pH values. So that, it is evident that diffusion or adsorption processes of the polymer at the

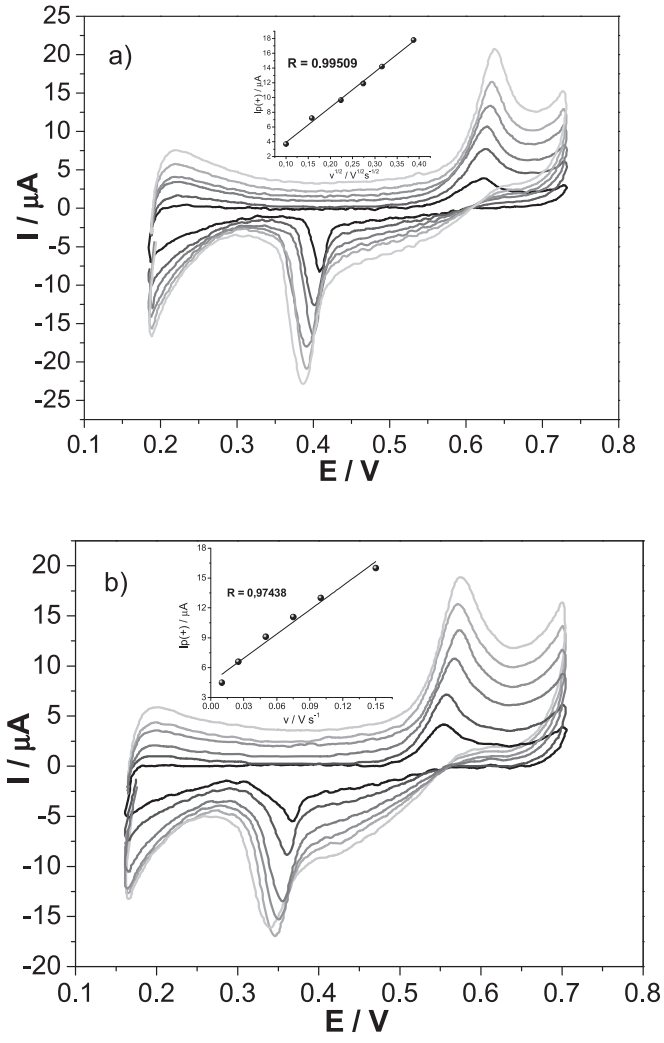

Fig. 1. Cyclic voltammograms for E100 at the water/1,2-dichloroethane interface. Aqueous phase composition: 1.0×10^{-2} M LiCl +0.100% w/v E100, (a) pH = 3.00 and (b) pH = 5.00. Organic phase composition: 1.0×10^{-2} M TPhAsDCC. v = 0.010, 0.025, 0.050, 0.075, 0.100 and 0.150 V s^{-1}.

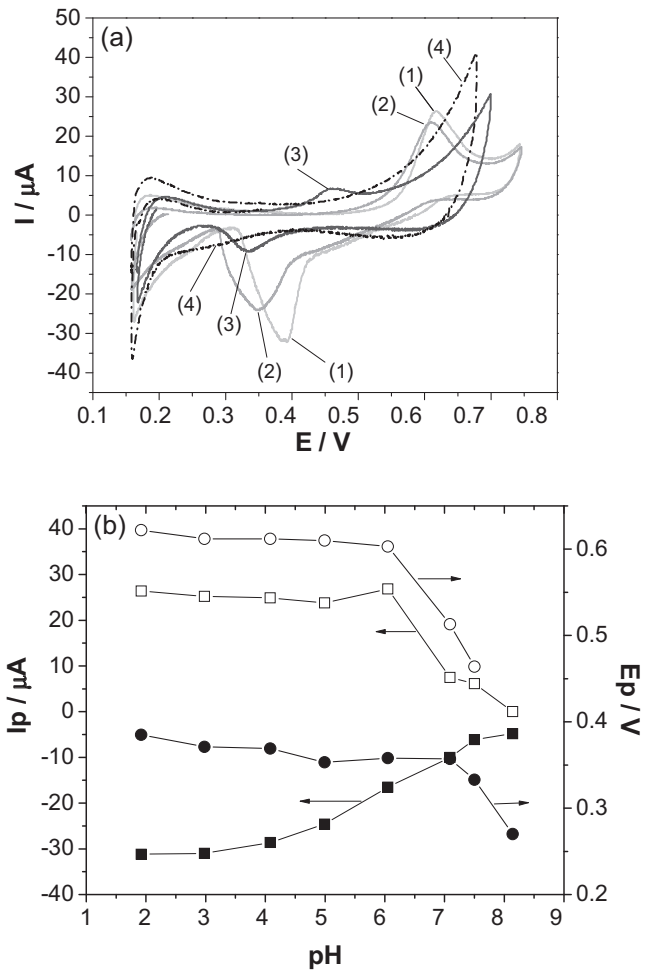

Fig. 2. (a) Cyclic voltammograms for E100 at the water/1, 2-dichloroethane interface recorded at different pH values: (1) 1.92; (2) 4.99; (3) 7.50; (4) 8.15. (b) Variation of $Ip(+)$ (□), $Ip(-)$ (■), $Ep(+)$ (○) and $Ep(-)$ (●) with pH value. Aqueous phase composition: 1.0×10^{-2} M LiCl +0.100% w/v E100, pH: from 1.92 to 8.15. Organic phase composition: 1.0×10^{-2} M TPhAsDCC. v = 0.050 V s^{-1}.

interface are taking place, and these two mechanisms are strongly dependent on the amount of positive charge in the structure of this polycation: when the charge on the polymer is high it is completely dissolved in aqueous phase and the diffusion process predominates, while as the positive charge decreases, the adsorption process prevails.

On the other hand, during the negative sweep, there is a sharp current peak, whose relationship $Ip(-)$ vs. $v^{1/2}$ is clearly not linear. Based on the peak shape, its dependence on the scan rate and the shift towards more negative potentials with increasing the scan rate, we postulate that this negative peak may be associated with an activation-controlled interfacial desorption mechanism.

Summing up, the evidences described above allow postulating that the transfer of E100, initially present in the aqueous bulk phase or adsorbed at the interface (depending on pH), to the organic phase takes place, during the positive scan, according to diffusion or activated-controlled process, respectively. Once the polymer is present at the organic side, it is adsorbed at the interface, probably via association with the anion of the organic electrolyte. When the potential sweep is reversed the desorption process and the returning of E100 to the aqueous phase occur, explaining in this way the general characteristics of the negative peak. Similar behavior was observed for polyquaternium 10 at the water/1,2-DCE interface [18].

3.1.1. *Effect of the pH*

As described in Section 1, the structure of polymer E100 contains tertiary amines, which can acquire positive charge by protonation. With the aim to analyze the effect of pH in the electrochemical response, E100, at concentration 0.100% w/v, was added to aqueous phases with different pH values within the range 1.92–8.15. The voltammograms obtained are shown in Fig. 2a. As it can be observed, at low pH values (voltammograms 1 and 2), the transfer process on the positive scan occurs approximately at E = 0.600 V, while the process in the negative scan is around to E = 0.400 V. When the pH increased (voltammograms 3) the shape of the i/E profile is drastically changed, evidencing a decrease in the peak current for both, positive and negative, processes together with a shift of peak potential towards lower values. At pH values greater than 7.50, the above mentioned transfer processes almost disappear (voltammograms 4).

Fig. 2b summarizes the variation of peak current values, $Ip(+)$ and $Ip(-)$, as well as peak potential values, $Ep(+)$ and $Ep(-)$, as a function of pH. It can be clearly observed that these parameters remain practically unchanged up to a pH value equal to 6.05, after which an abrupt decay is evident.

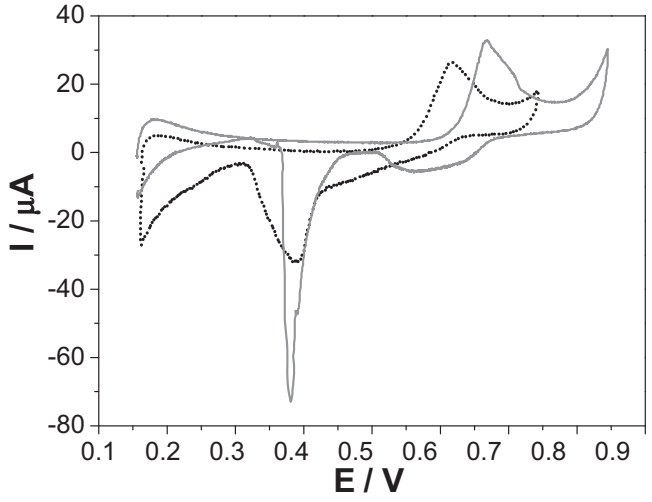

Fig. 3. Cyclic voltammograms for E100 at $\nu = 0.050\ V\ s^{-1}$ using different organic electrolytes. Aqueous phase composition: 1.0×10^{-2} M LiCl +0.100% w/v E100, pH = 3.00. Organic phase composition: (···) 1.0×10^{-2} M TPhAsDCC; (—) 1.0×10^{-2} M TPnATClPhB.

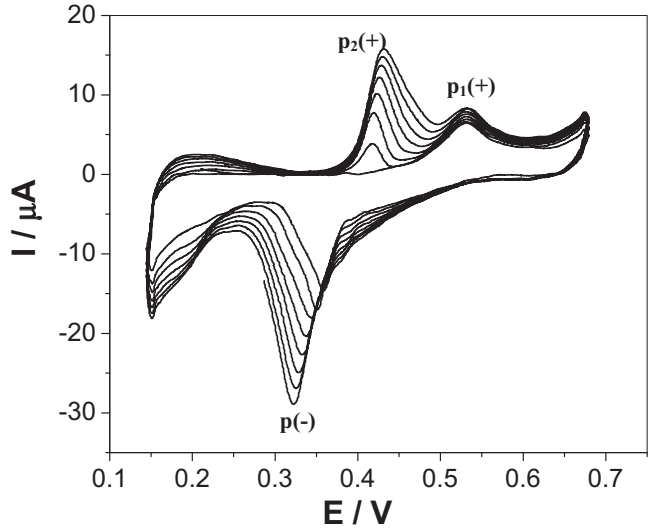

Fig. 4. Repetitive cyclic voltammograms applied to the interface at $\nu = 0.050\ V\ s^{-1}$. Aqueous phase composition: 1.0×10^{-2} M LiCl +0.050% w/v E100, pH = 4.08. Organic phase composition: 1.0×10^{-2} M TPhAsDCC.

Concerning to the transfer process observed when polyelectrolytes are present in aqueous phase two mechanisms are plausible during the positive scan: (a) transfer of the polymer from the aqueous to the organic phase followed by complex formation with the organic anion, or (b) transfer of organic anion from the organic to the aqueous phase followed by association with the polyelectrolyte, according to the mechanism suggested by MD Scanlon et al., for the electrochemical behavior of lysozyme at the water/1,2-dichloroethane [37]. The dependence of the electrochemical response with the pH variation, shown in Fig. 2a and b, suggests that option (a) is operative in this case, since the increase of pH results in a decrease in the total charge of the polymer, which leads, on one hand, to a decrease of the current, which is proportional to the charge transferred and, on the other hand, to a decrease in peak potential values associated with the increased hydrophobicity of the polymer as its net charge is reduced. In this case, the processes observed could not be attributed to the facilitated transfer of the organic anion, due to the presence of the polymer in the aqueous phase (option b), since if this were the mechanism, it should be noted an increase in *Ep*(+) values as pH increases.

Moreover, from the results shown in Fig. 2b a p*K*a value, for the amino groups of the polymer, equal to 6.85 could be estimated from the point of *Ip*(+) value equal to the half of the initial value, i.e., the pH at which protonated species fraction equals to that of neutral species. This p*K*a value is close to 7.0–7.3, p*K*a corresponding to 2-(diethylamino)ethyl metacrylate homopolymer (PDEA) [38].

3.1.2. Effect of the organic electrolyte

Fig. 3 compares the voltammetric profiles obtained for 0.100% w/v E100 in aqueous phase and two different base electrolytes in organic phase at a concentration 1.0×10^{-2} M: TPhAsDCC and TPnATClPhB. As it can be noted, the transfer of E100 occurs at different potential values depending on the electrolyte present in organic phase, being the lowest transfer potential obtained in the presence of DCC^-, so that the supporting electrolyte of the organic phase is directly related to the transfer of the polymer, probably, through the formation of ion pairs between the anion of the organic salt and the positive amine groups in E100 after the transfer of the polymer to the organic phase. Therefore, E100 transfer is observed at a higher potential when $TClPhB^-$ anion is used as supporting electrolyte of the organic phase, whose accumulation at the interface occurs at higher potentials than DCC^-.

This result demonstrates the involvement of the organic anion in E100 transfer, confirming the hypothesis that the positively charged polymer (dissolved or adsorbed) is electrochemically transferred from the aqueous to the organic phase, followed by the formation of ion pairs with the anion of the organic salt.

The above affirmation is similar to that concluded by Trojanék et al. [28] for protamine transfer at a liquid/liquid interface, who observed that the peak potential depends on the nature of the organic electrolyte. The authors attributed this effect to the ion pair interactions between the protamine polycation and the organic electrolyte anion, and found that the stability of the ion pair decreases with increasing the size of the anion. Correlating this prior information to our results, we can explain the differences observed in the negative potential sweep when using either of the organic anions. As can be noted in Fig. 3, during the reverse scan, the negative peak observed in presence of TPnATClPhB is sharper than the corresponding for TPhAsDCC, which would indicate a faster desorption process for E100 when TPnATClPhB is used as organic electrolyte, revealing a lower stability of the ion pair formed by the anion $TClPhB^-$ and the amine groups of E100 at the organic side of the interface. Nevertheless, the negative peak potential is the same regardless of the nature of the organic electrolyte, confirming that this process corresponds to the polymer desorption and its transfer from the organic side of the interface to the aqueous phase.

3.1.3. Effect of successive potentiodynamic cycles

Fig. 4 shows the result obtained when successive potentiodynamic cycles are applied to the interface. In this experiment, E100 was present in the aqueous phase at a concentration 0.050% w/v and the pH was 4.08, while the organic phase contained the organic electrolyte TPhAsDCC at a concentration 1.0×10^{-2} M. As it can be observed, only the above described electrochemical process around $E = 0.530\ V$ ($p_1(+)$) on the forward scan during the first cycle and a negative peak ($p(-)$) at $E = 0.350\ V$, on the reverse scan, are evident. These two processes were assigned in Section 3.1 to the transfer of E100 (adsorbed or dissolved, depending on pH) from the aqueous to the organic phase, followed by ion pair formation with the organic anion and adsorption at the organic side of the interface during the positive sweep, and the desorption of E100 returning to aqueous phase during the reverse scan. Upon subsequent scans, a new peak appears at $E = 0.400\ V$ ($p_2(+)$) whose current increases as the number of cycles performed increases, whereas the

pre-existing peak $p_1(+)$ remains unchanged with successive sweeps. Interestingly, although two electrochemical processes are observed on the forward scan, only one peak, p(−), is observed for the reverse scan. However, the intensity of this peak increases with the number of scans while the peak potential is shifted to more negative values.

The new transfer process, $p_2(+)$, which occurs since the second cycle, must correspond to a new species generated during the first potential scan, and whose formation continues taking place in the successive sweeps, leading to the increase in current values with cycling.

It is important to remark that both the peak potential and the peak current corresponding to the process $p_1(+)$ are held constant during successive cycles, which is in agreement with the behavior of species that are transferred by a diffusion control mechanism as it was stated above under these experimental conditions (pH < 5). Furthermore, the increase in current for the negative process p(−) with the number of cycles, indicates that both species transferred in the positive sweep are desorbed at the same potential during the negative sweep.

Taking into account these results, the transfer mechanism proposed for this polyelectrolyte is summarized in the following equations:

First cycle:

$$p_1(+): \quad P^{z+}_{(w,ads,dis)} + nDCC^{-}_{(o)} \rightarrow P(DCC)^{(z-n)+}_{n(o,ads)} \tag{1}$$

$$p_1(-): \quad P(DCC)^{(z-n)+}_{n(o,ads)} \rightarrow P(DCC)^{(z-x)+*}_{x(w,ads,dis)} + (n-x)DCC^{-}_{(o)} \tag{2}$$

Second and successive cycles:

$$p_2(+): \quad P(DCC)^{(z-x)+*}_{z(w,ads,dis)} \rightarrow P(DCC^{-})^{(z-n)+}_{x(o,ads)} \tag{3}$$

That is, during the positive sweep of the first cycle, the positively charged molecules of E100 (P^{z+}), dissolved in solution together with a small fraction of P^{z+} molecules adsorbed at the aqueous side interface, are transferred, (Eq. (1)). Once P^{z+} molecules are at the organic side, their adsorption at the interface occurs via the formation of ion-pairs between positive groups of E100 and the organic anion, DCC^{-}, as it was described above.

During the negative sweep the polymer returns to the aqueous phase, however, the returning species are not completely equal to the polymer initially transferred, P^{z+}. This may be due to conformational changes in the structure, or to the fact that during the desorption process some molecules of the organic anion remain associated to the polymer, thus generating the species $P(DCC)^{(z-x)+*}$. This new species, identified with an asterisk, may be present as dissolved in the aqueous phase or adsorbed in the aqueous side interface, and their transfer to the organic phase is the responsible for the process $p_2(+)$ observed in the second and subsequent cycles.

Fig. 5a shows the variation of peak current for the processes $p_2(+)$ and p(−), with the number of cycles performed, at different values of pH in the aqueous phase. It is observed that the increase of cycles number produces always an increase in *Ip*, which is more important when the polymer charge is higher (low pH values).

Fig. 5b shows the effect of the sweep rate, the pH and the number of cycles on *Ep* for the processes $p_2(+)$ and p(−). As it can be noted the peak potential for $p_2(+)$ remains almost constant for both pH values (1.02 and 4.08) provided that the potential sweeps are performed at low scan rate, but it shifts slightly towards more positive values when the cycles are carried out at a higher sweep rate. For the desorption process, it can be observed that *Ep* shifts towards more negative potentials after successive cycles, indicating that a stabilization of the adsorbed species was produced, retarding their desorption. This effect is more noticeable at higher pH values and higher sweep rates, denoting that the desorption process is slow.

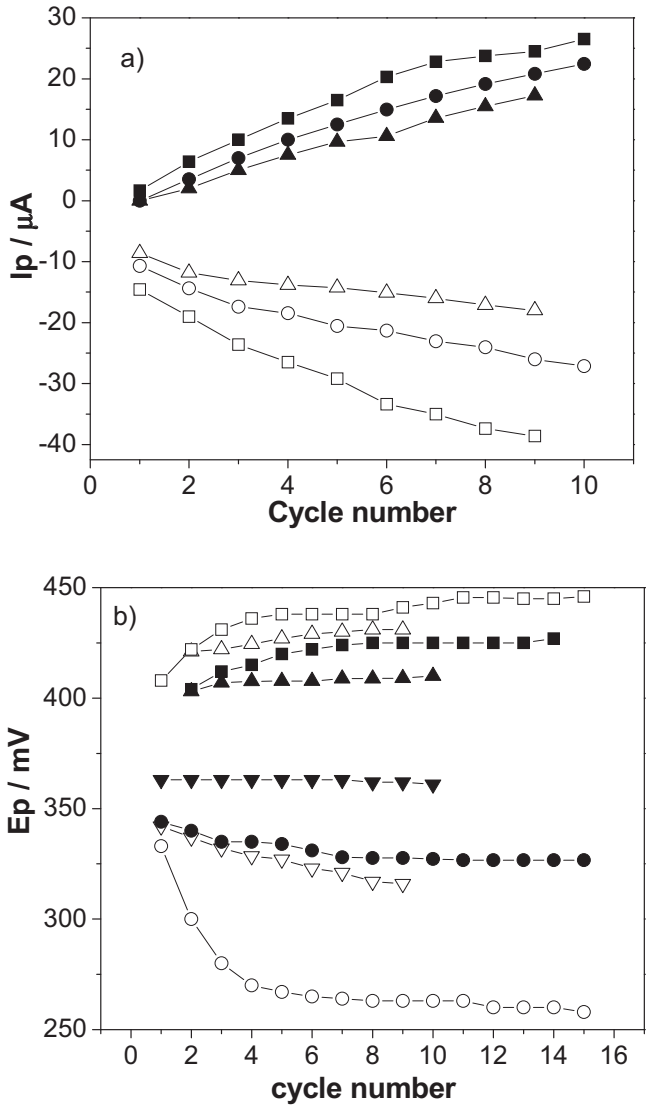

Fig. 5. (a) Variation of *Ip* with the number of cycles for the processes $p_2(+)$ (closed symbols) and p(−) (open symbols). Aqueous phase composition: 1.0×10^{-2} M LiCl +E100 0.050% w/v, pH: (■, □) 1.20; (●, ○) 3.03; (▲, △) 4.08. Organic phase composition: 1.0×10^{-2}M TPhAsDCC. $\nu = 0.010\,V\,s^{-1}$. (b) Variation of *Ep* with the number of cycles for the processes $p_2(+)$ (▲, ■, △, □) and $p(-)$ (▼, ●,▽, ○) at pH = 1.02 (closed symbols), and pH = 4.08 (open symbols). Aqueous phase composition: 1.0×10^{-2} M LiCl +E100 0.050% w/v. (a) $\nu = 0.010\,V\,s^{-1}$, (b) $\nu = 0.050\,V\,s^{-1}$ (●, ■, ○, □) or $\nu = 0.010\,V\,s^{-1}$, (▲, ▼, △,▽).

3.1.4. Potential step followed by negative linear sweep

To analyze the effect of the sweep rate in the negative scan, $\nu_{(-)}$, under controlled interfacial conditions, potential steps at $E_{step} = 0.580$ and 0.640 V were applied to the interface during different times, $\Delta\tau$, prior to desorption during the negative scan. The voltammograms obtained (negative sweeps) show a shift in the peak potential towards negative values as $\Delta\tau$ increases and, therefore, the amount of polymer adsorbed at the interface (data not shown). This result would indicate an attractive interaction between the adsorbed species.

Fig. 6 compares the effect of $\Delta\tau$ on the negative peak potential, $Ep(-)$, for two different values of E_{step} and $\nu_{(-)} = 0.010$ or $0.050\,V\,s^{-1}$. As mentioned above, $Ep(-)$ shifts towards more negative potentials with increasing $\Delta\tau$, indicating that the desorption process becomes irreversible by increasing the amount of adsorbed polymer or that attractive interactions exist between the adsorbed molecules. This

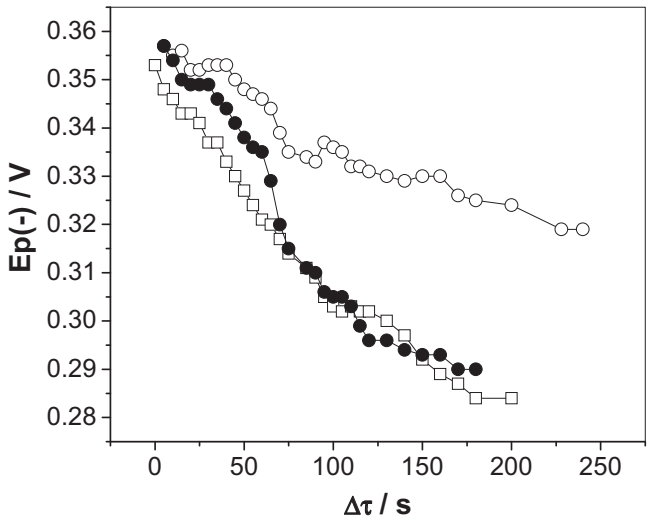

Fig. 6. Variation of $Ep(-)$ with step time, $\Delta\tau$, for negative scans recorded after performing a potential step at E_{step} = 0.580 V (○, ●) or 0.640 V (□). ν = 0.010 V s^{-1} (○, □) or 0.050 V s^{-1} (●). Aqueous phase: 1.0 × 10^{-2} M LiCl +E100 M 0.020% w/v. Organic phase composition: 1.0 × 10^{-2} M TPhAsDCC.

effect becomes more important when E_{step} and $\nu_{(-)}$ increase, as occurring in quasi-reversible adsorption/desorption processes.

Taking into account the above considerations, we select the conditions $\nu_{(-)}$ = 0.010 V s^{-1} to carry out an analysis of the desorption charge, $q(-)$, since this low ν value ensures the complete desorption during the negative scan. In this way, $q(-)$ values were calculated by integrating the desorption peak, during the negative sweep recorded at $\nu_{(-)}$ = 0.010 V s^{-1}, after holding the interfacial potential at E_{step} = 0.580 or 0.640 V during different times, $\Delta\tau$. The results are shown in Fig. 7 where it can be clearly observed the presence of a *plateau* and three inflection points, highlighted with horizontal dotted lines, under conditions of E_{step} = 0.580. The $q(-)$ value corresponding to the first plateau is approximately equal to 42.5 μC, and it probably occurs due to the saturation of the available adsorption sites at the interface. Then, the charge increases again to reach another constant value, or inflection point, at approximately 80.0 μC, and this behavior is repeated again for q = 120 and 160 μC. The fact that the charge is stabilized always at values multiples of 40 μC may be due to the formation of multilayers when the polymer is adsorbed. If an average molecular area equal

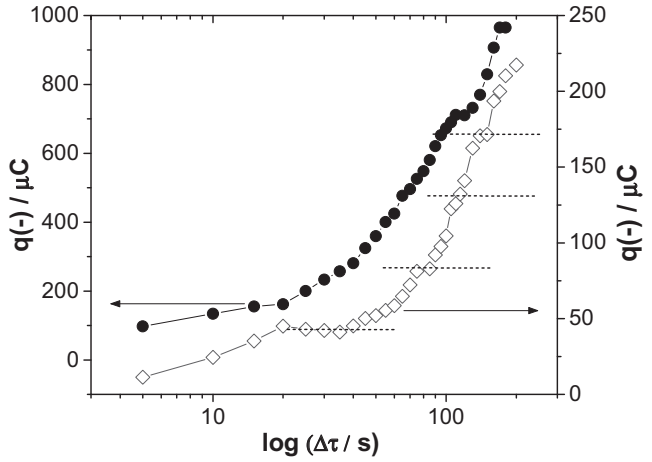

Fig. 7. Charge values corresponding to desorption process of E100, $q(-)$, as a function of step time, $\Delta\tau$. E_{step} = 0.580 V (◊) or 0.640 V (●). Aqueous phase: 1.0 × 10^{-2} M LiCl +E100 0.020% w/v. Organic phase composition: 1.0 × 10^{-2} M TPhAsDCC. ν = 0.010 V s^{-1}.

Table 1
f values calculated for different concentrations of E100 and different scan rates.

c_{E100} (% w/v)	ν (V s^{-1})	f
0.02	0.01	−3.73
0.02	0.05	−6.84
0.05	0.01	−4.73
0.05	0.05	−6.73

to 7000 Å for E100 is considered, which was determined from pressure-molecular area isotherms at a water/air interface (data not shown), and taking into account the total charge per molecule in the polymer (n = 571), a theoretical charge value corresponding to a monolayer of E100, equal to 23.5 μC, can be calculated. This value, lower than that obtained from voltammetric results, indicates that the area occupied by the polymer at the polarized liquid/liquid interface is lower than at the water/air interface, which can be explained taking into account the neutralization of charged amino groups, by DCC^- anions at the organic side of the interface, which reduces electrostatic repulsions, allowing a more efficient packaging.

On another hand, a quite different response is obtained when E_{step} = 0.640 V. In this case, the desorption charge increases continuously, probably due to the fact that, at these higher potential values, the polymer continuously adsorbs without giving rise to the formation of successive layers of adsorption.

As mentioned above, the variation of $Ep(-)$ with $\Delta\tau$ and $\nu_{(-)}$ suggests an attractive interaction between the adsorbates, thus explaining the shift of $Ep(-)$ towards more negative values, with increasing both experimental variables. So that, the Roginsky–Zeldovich isotherm, which relates interfacial coverage (θ) with log $\Delta\tau$ [39–41]:

$$\theta = k + \frac{2.3}{\alpha f} \log \Delta\tau \quad (4)$$

is relevant in this case. In Eq. (4), f is the lateral interaction parameter, which represents the variation of the free energy of adsorption with respect to the variation of θ and α is the charge transfer coefficient. Values of $f > 0$ indicate that ΔG^0_{ads} increases with the coverage, i.e., the adsorption process is inhibited at high coverages, existing repulsion between adsorbate molecules. On the other hand, values of $f < 0$, indicate that the adsorption process is facilitated by the attractive interactions between the adsorbed molecules. The interfacial coverage, θ, is defined as the ratio between the amount of adsorbed species, m^{Ads}, and those necessary for a monolayer formation, m^*. When charged species are involved, m^{Ads} and m^* are transformed into q^{Ads} and q^*, respectively, and θ is defined by the following equation:

$$\theta = \frac{q^{Ads}}{q^*} \quad (5)$$

Therefore, θ values were calculated by dividing the charge values corresponding to the desorption process, for each $\Delta\tau$, by the charge value for a monolayer formation, i.e., q^* = 42.5 μC for E_{step} = 0.580 V and $\nu_{(-)}$ = 0.010 V s^{-1}. The resulting θ values were plotted versus log $\Delta\tau$, obtaining a linear relationship, according to equation (4) (data not shown). Thus, the parameter f was evaluated from the slope of θ vs. log $\Delta\tau$ graphics, and the results obtained for two E100 concentrations and two different $\nu_{(-)}$ are listed in Table 1.

The values of $f < 0$ indicate a strong attraction between the adsorbed species at the interface and a stabilization with $\Delta\tau$, explaining hence the reason for which the desorption process is slow. These attractive intermolecular forces are due to van der Waals interactions between permanent dipoles in E100 molecules. As it can also be noted in Table 1, the f values for both polymer concentrations, are quite similar, while those obtained for different $\nu_{(-)}$ are markedly distinct. This fact reveals that the desorption

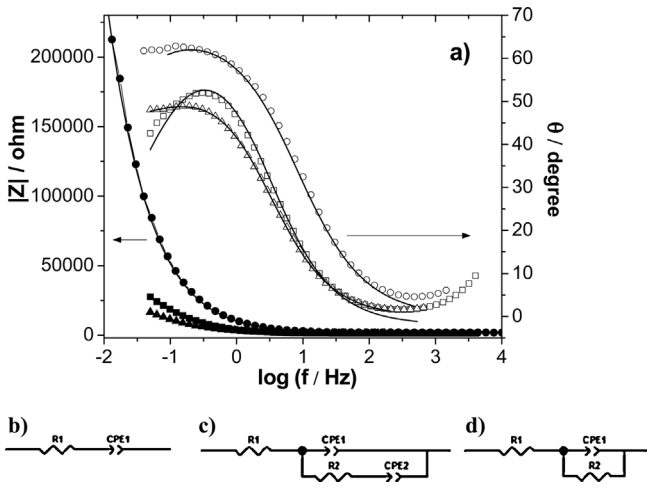

Fig. 8. (a) Bode plots, log $|Z|$ (close symbols) and phase angle θ (open symbols), vs. log$f$, obtained in absence of E100 at E_{dc} = 0.450 V (○, ●) and in presence of 0.020% w/v E100 at E_{dc} = 0.530 V (△, ▲) or E_{dc} = 0.450 V after performing four successive potentiodinamic cycles (□, ■). Fitting results are shown in solid line. Aqueous phase composition: 1.0×10^{-2} M LiCl +0.020% w/v E100. Organic phase composition: 1.0×10^{-2} M TPhAsDCC. (b)–(d) Equivalent circuits employed to fit EIS results. Circuit elements: solution resistance $R1$; constant phase elements CPE1 and CPE2 corresponding to double layer capacity and Warburg impedance, respectively; charge transfer resistance $R2$.

process is incomplete at high scan rates, leading to overestimated values of f, typical of a slow process.

3.2. Electrochemical impedance spectroscopy (EIS)

With the aim of completing the characterization of the interfacial processes $p_1(+)$ and $p_2(+)$ and in order to corroborate the proposed mechanism, impedance spectra were recorded at $E_{dc} = Ep_1(+)$ and $Ep_2(+)$ in a frequency range, f, between 0.03 and 3000 Hz.

Fig. 8a shows the typical Bode graphs, recorded in the absence and the presence of E100. The experimental results were fitted employing the equivalent circuits schematized in Fig. 8b–d, and the best fitting obtained between the theoretical and experimental data, in each case, was selected to explain the results. A constant phase element (CPE), instead of pure capacitance and/or Warburg impedance, was introduced in all of the circuits. The impedance of a constant phase element is defined as [42,43]:

$$Z_{CPE} = [Q(j\omega^n)^{-1}] \quad \text{with} \quad -1 \le n \le 1 \tag{6}$$

where Z_{CPE} ($\Omega\,cm^2$) is the impedance, the constant Q ($\Omega^{-1}\,s^n\,cm^{-2}$) is a combination of properties related to both the interface and the electroactive species and is independent of frequency. The exponent n is related to the slope of log $|Z|$ vs. log$f$ Bode plot, i.e., to the phase angle, θ, by the relation $n = 2\theta/\pi$, and $j = (-1)^{0.5}$.

The spectra recorded at E_{dc} = 0.450 V ($Ep_2(+)$), in the absence of the polymer, was best fitted employing the equivalent circuit shown in Fig. 8b, containing a resistance $R1 = (1937 \pm 9)\,\Omega$, corresponding to the solution resistance, in series with a CPE, with a value of $n = 0.7787 \pm 0.0002$, corresponding to the double layer capacity, with a value $C_{dl} = (2.46 \pm 0.02) \times 1\,0^{-5}$ F.

The impedance spectra obtained when E100 is present in the aqueous phase, are dependent on the E_{dc} applied. At E_{dc} = 0.550 V ($Ep_1(+)$), the Bode plots were best fitted with the equivalent circuit shown in Fig. 8c, in which the resistor $R1 = (1355 \pm 3)\ \Omega$ corresponds to the solution resistance, and the components in parallel, represent two processes occurring simultaneously: on the one hand, the CPE1 with a coefficient value $n = 0.86 \pm 0.06$, corresponds to double layer capacity, with a value $C_{dl} = (6.5\ \pm 0.2) \times 10^{-5}\ F$; while the elements $R2 = (1.0 \pm 0.4) \times 103\,\Omega$ and CPE2, with a value of $n = 0.44 \pm 0.02$, represent the charge transfer resistance and the Warburg impedance, respectively, indicating the presence of a diffusion process, which agrees with the results obtained by cyclic voltammetry. Finally, the impedance spectra obtained in presence of E100 at E_{dc} = 0.450 V ($Ep_2(+)$), after performing four successive potential cycles, to ensure the occurrence of process $p_2(+)$, were best fitted employing the circuit shown in Fig. 8d. As in the previous cases, $R1$ represents the solution resistance, $R1 = (1399 \pm 8)\,\Omega$ and CPE1, with a coefficient value of $n = 0.797 \pm 0.005$ corresponds to double layer capacity, $C_{dl} = (6.8 \pm 0.2) \times 10^{-5}$ F. The element $R2$, in parallel, is due to the charge transfer resistance. The presence of $R2$ and the absence of the Warburg impedance in this equivalent circuit may be associated with an interfacial transfer process of adsorbed molecules, not controlled by diffusion.

Finally, it is worthwhile noting that C_{dl} values obtained in the presence of the polymer are higher than those in its absence, certainly due to the increase of interfacial charge, and also evidenced in the voltammograms in Fig. 1 by the increase in background current on reverse scans at potentials values previous to the corresponding to desorption of the polymer.

4. Conclusions

The results obtained enable to postulate a mechanism of adsorption/diffusion control for the transfer of the polyelectrolyte E100 at the water/1,2-DCE interface. Important differences were observed between the first and the subsequent potential sweep in the voltammograms. During the first cycle, a single positive current peak, and its corresponding negative one, were observed, whose $Ep(+)$ and $Ip(+)$ decreased as the pH of aqueous phase increased. This dependence suggests that polymer molecules are transferred from the aqueous to the organic phase, and the variation of $Ip(+)$ with ν revealed that diffusion or adsorption processes of the polymer at the interface can take place, depending on the pH of the aqueous phase. Once E100 is transferred to the organic side, it adsorbs at the interface via formation of ion pairs with the anions DCC^- and the desorption process takes place during the negative sweep. On another hand, a second process, previous to the transfer controlled by diffusion, appears during the second and successive potential scans, attributable to the transfer of some species, which were not present during the first cycle. It was concluded that this kind of species could be due to conformation changes in E100 molecules, due to the adsorption–desorption process, or to the retaining of DCC^- ions in the positive sites of the polyelectrolyte after the desorption process. This new conformation of the polymer favors its spontaneous adsorption at the interface producing, from the second cycle, a pre-peak attributable to the transfer of these adsorbed species. This process is favored by increasing the number of cycles and decreasing pH. Even in this case, a single peak, attributable to the desorption of the polymer, is observed in the reverse scan. The analysis of the desorption process, allowed the determination of the lateral interaction parameter.

In this way, the combination of cyclic voltammetry and EIS at liquid/liquid interfaces, demonstrated to be a valid tool to evaluate the state of polymers at these interfaces.

Acknowledgments

Financial support from Consejo Nacional de Investigaciones Científicas y Tecnológicas (CONICET), Agencia Nacional de Promoción Científica y Tecnológica (FONCyT) and Secretaría de Ciencia y Técnica de la Universidad Nacional de Córdoba (SECyT) is gratefully acknowledged. J.S. Riva wishes to thank CONICET for the

fellowships awarded. D. Beltramo and L.M. Yudi are members of the Research Career of CONICET.

References

[1] R.I. Moustafine, V.A. Kemenova, G. Van den Mooter, Characteristics of interpolyelectrolyte complexes of Eudragit E100 with sodium alginate, International Journal of Pharmaceutics 294 (2005) 113–120.

[2] R.I. Moustafine, I.M. Zaharov, V.A. Kemenova, Physicochemical characterization and drug release properties of Eudragit® E PO/Eudragit® L 100-55 interpolyelectrolyte complexes, European Journal of Pharmaceutics and Biopharmaceutics 63 (2006) 26–36.

[3] D.A. Quinteros, V. Ramirez Rigo, A.F. Jimenez Kairuz, M.E. Olivera, R.H. Manzo, D.A. Allemandi, Interaction between a cationic polymethacrylate (Eudragit E100) and anionic drugs, European Journal of Pharmaceutical Sciences 33 (2008) 72–79.

[4] M.L. Guzmán, R.H. Manzo, M.E. Olivera, Eudragit E100 as a drug carrier: the remarkable affinity of phosphate ester for dimethylamine, Molecular Pharmaceutics 9 (2012) 2424–2433.

[5] R.C. Rowe, P.J. Sheskey, S.C. Owen, Polymethacrylates, in: Handbook of Pharmaceutical Excipients, fifth ed., American Pharmaceutical Association and Pharmaceutical Press, London, 2006, pp. 525–533.

[6] V.M. Rao, K. Engha, Y. Qiu, Design of pH-independent controlled release matrix tablets for acidic drugs, International Journal of Pharmaceutics 252 (2003) 81–86.

[7] R. Kalaiselvan, G.P. Mohanta, P.K. Manna, A. Manimakalai, Solid-phase preparation and characterization of albendazole solid dispersion, ARS Pharmaceutica 47 (2006) 91–107.

[8] H. Valizadeh, P. Zakeri-Milani, M. Barzegar-Jalali, G. Mohammadi, M. Danesh-Bahreini, K. Adibkia, A. Nokhodchi, Preparation and characterization of solid dispersions of piroxicam with hydrophilic carriers, Drug Development and Industrial Pharmacy 33 (2007) 45–56.

[9] P.D. Sawant, D. Luu, R. Ye, R. Buchta, Drug release from hydroethanolic gels: effect of drug's lipophilicity (log *P*), polymer–drug interactions and solvent lipophilicity, International Journal of Pharmaceutics 396 (2010) 45–52.

[10] Y. Hu, Y. Wu, X.J. Xia, Z. Wu, W.Q. Liang, J. Gao, Development of drug-in-adhesive transdermal patch for α-asarone and in vivo pharmacokinetics and efficacy evaluation, Drug Delivery 18 (2011) 84–89.

[11] R.V. Alasino, S.F. Ausar, I.D. Bianco, L.F. Castagna, M. Contigiani, D.M. Beltramo, Amphipathic and membrane-destabilizing properties of the cationic acrylate polymer Eudragit® E100, Macromolecular Bioscience 5 (2005) 207–213.

[12] R.V. Alasino, I.D. Bianco, M.S. Vitali, J.A. Zarzur, D.M. Beltramo, Characterization of the inhibition of enveloped virus infectivity by the cationic acrylate polymer Eudragit E100, Macromolecular Bioscience 7 (2007) 1132–1138.

[13] L. Zhang, Y. Kitazumi, T. Kakiuchi, Potential-dependent adsorption and transfer of poly(diallyldialkylammonium) ions at the nitrobenzene|water Interface, Langmuir 27 (2011) 13037–13042.

[14] S. Ulmeanu, H.J. Lee, H.H. Girault, Voltammetric characterisation of polyelectrolyte adsorption/transfer at the water|1,2-DCE interface, Electrochemistry Communications 3 (2001) 539–543.

[15] H. Katano, I. Kameoka, Y. Murayama, H. Tatsumi, T. Tsukatani, M. Makino, Voltammetric study of the transfer of polyammonium ions at nitrobenzene/water interface, Analytical Sciences 20 (2004) 1581–1585.

[16] S. Hakkarainen, S.L. Gilbert, A.K. Kontturi, K. Kontturi, Amperometric method for determining the degree of complexation of polyelectrolytes with cationic surfactants, Journal of Colloid and Interface Science 272 (2004) 404–410.

[17] J.S. Riva, A.V. Juárez, D.M. Beltramo, L.M. Yudi, Interaction of chitosan with mono and divalent anions in aqueous solution studied by cyclic voltammetry at a water/1,2-dichloroethane interface, Electrochimica Acta 59 (2012) 39–44.

[18] J.S. Riva, K. Bierbrauer, D.M. Beltramo, L.M. Yudi, Electrochemical study of the interfacial behavior of cationic polyelectrolytes and their complexation with monovalent anionic surfactants, Electrochimica Acta 85 (2012) 659–664.

[19] M. Calderón, L.M.A. Monzón, A.V. Juarez, M. Martinelli, M. Strummia, L.M. Yudi, Electrochemical study of a dendritic family at the water/1,2-dichloroethane interface, Langmuir 24 (2008) 6343–6350.

[20] J.S. Riva, R. Iglesias, L.M. Yudi, Electrochemical adsorption of a cationic cellulosic polymer by ion pair formation at the interface between two immiscible electrolyte solutions, Electrochimica Acta 17 (2013) 584–591.

[21] Z. Samec, A. Trojanek, J. Langmaier, E. Samcova, Cyclic voltammetry of biopolymer heparin at PVC plasticized liquid membrane, Electrochemistry Communications 5 (2003) 867–870.

[22] J. Guo, Y. Yuan, S. Amemiya, Voltammetric detection of heparin at polarized blood plasma/1,2-dichloroethane interfaces, Analytical Chemistry 77 (2005) 5711–5719.

[23] J. Guo, S. Amemiya, Voltammetric heparin-selective electrode based on thin liquid membrane with conducting polymer-modified solid support, Analytical Chemistry 78 (2006) 6893–6902.

[24] P.J. Rodgers, P. Jing, Y. Kim, S. Amemiya, Electrochemical recognition of synthetic heparin mimetic at liquid/liquid microinterfaces, Journal of American Chemical Society 130 (2008) 7436–7442.

[25] P.J. Rodgers, P. Jing, Y. Kim, S. Amamiya, Voltammetric extraction of heparin and low-molecular-weight heparin across 1,2-dichloroethane/water interfaces, Langmuir 25 (2009) 13653–13660.

[26] S. Amemiya, X. Yang, T.L. Wazenegger, Voltammetry of the phase transfer of polypeptide protamines across polarized liquid/liquid interfaces, Journal of American Chemical Society 125 (2003) 11832–11833.

[27] Y. Yuan, S. Amemiya, Facilitated protamine transfer at polarized water/1,2-dichloroethane interfaces studied by cyclic voltammetry and chronoamperometry at micropipet electrodes, Analytical Chemistry 76 (2004) 6877–6886.

[28] A. Trojanék, J. Langmaier, E. Samcova, Z. Samec, Counterion binding to protamine polyion at a polarised liquid–liquid interface, Journal of Electroanalytical Chemistry 603 (2007) 235–242.

[29] M. Shinshi, T. Sugihara, T. Osakai, M. Goto, Electrochemical extraction of proteins by reverse micelle formation, Langmuir 22 (2006) 5937–5944.

[30] F. Kivlehan, Y.H. Lanyon, D.W.M. Arrigan, Electrochemical study of insulin at the polarized liquid–liquid interface, Langmuir 24 (2008) 9876–9882.

[31] G. Herzog, P. Eichelmann-Daly, D.W.M. Arrigan, Electrochemical behaviour of denatured haemoglobin at the liquid/liquid interface, Electrochemistry Communications 12 (2010) 335–337.

[32] G. Herzog, M.T. Nolan, D.W.M. Arrigan, Haemoglobin unfolding studies at the liquid–liquid interface, Electrochemistry Communications 13 (2011) 723–725.

[33] S. O'ullivan, D.W.M. Arrigan, Electrochemical behaviour of myoglobin at an array of microscopic liquid–liquid interfaces, Electrochimica Acta 77 (2012) 71–76.

[34] M.A. Mendez, Z. Nazemi, I. Uyanik, H.H. Girault, Melittin adsorption and lipid monolayer disruption at liquid–liquid interfaces, Langmuir 27 (2011) 13918–13924.

[35] T. Osakai, Y. Yuguchi, E. Gohara, H. Katano, Direct label-free electrochemical detection of proteins using the polarized oil/water interface, Langmuir 26 (2010) 11530–11537.

[36] A.M. Baruzzi, J. Uhlken, Current interruption potentiostat for elimination of the IR drop in four-electrode systems, Journal of Electroanalytical Chemistry 282 (1991) 267.

[37] M.D. Scanlon, E. Jennings, D.W.M. Arrigan, Electrochemical behaviour of hen-egg-white lysozyme at the polarisedwater/1, 2-dichloroethane interface, Physical Chemistry Chemical Physics 11 (2009) 2272–2280.

[38] J.I. Amalvy, E.J. Wanless, Y. Li, V. Michailidou, S.P. Armes, Synthesis and characterization of novel pH-responsive microgels based on tertiary amine methacrylates, Langmuir 20 (2004) 8992–8999.

[39] V.S. Bagotzky, Yu.B. Vassiliev, Adsorption of organic substances on platinum electrodes, Electrochimica Acta 11 (1966) 1439–1461.

[40] V.S. Bagotzky, Yu.B. Vassiliev, Mechanism of electro-oxidation of methanol on the platinum electrode, Electrochimica Acta 12 (1967) 1323–1343.

[41] S.Z. Roginsky, J.B. Zeldovich, The catalytic oxidation of carbon monoxide on manganese dioxide, Acta Physiochimica USSR 1 (1934) 554.

[42] N.P. Cosman, K. Fatih, S.G. Roscoe, Electrochemical impedance spectroscopy study of the adsorption behaviour of α-lactalbumin and β-casein at stainless steel, Journal of Electroanalytical Chemistry 574 (2005) 261–271.

[43] A. Boukamp, Equivalent Circuit, University of Twente, Enschede, The Netherlands, 1989, pp. 12.